Contaminant Leaching from Saltstone

By

J.C. Seaman*, F.M. Coutelot**, J. Cochran***,

R.J. Thomas**** and M.R. Baker****

*Senior Research Scientist
Assistant Director – Research/Quality Assurance
Savannah River Ecology Laboratory
The University of Georgia
Aiken, SC 29802
Phone: 803-725-0977
seaman@srel.uga.edu

**Assistant Research Scientist
coutelot@uga.edu

***SREL Research Professional
cochraj@uga.edu

****Graduate Student Assistants
rjthomas@srel.uga.edu
mrbaker@srel.uga.edu

REVIEWS AND APPROVALS

Authors:

John C. Seaman, SREL Associate Director-Research Senior Research Scientist — Date: 9/29/16

Review:

Gary Mills, PhD
SREL Research Scientist — Date: 9-29-16

Approval:

Steven Simner, CTF Savannah River Remediation LLC — Date: 9/29/2016

Table of Contents

EXECUTIVE SUMMARY

At the Department of Energy's (DOE) Savannah River Site (SRS) chemically reducing materials, such as blast furnace slag (BFS), are added to grout formulations mixed with low-level radioactive salt waste solutions in order to enhance the attenuation of redox sensitive contaminants (e.g., technetium-99 (^{99}Tc)). The resulting cementitious material, known as *saltstone*, is deposited in a series of concrete vaults, referred to as Saltstone Disposal Units (SDUs) for long-term disposal at the Saltstone Disposal Facility (SDF). Such chemically reducing grouts provide both a physical (i.e., low saturated hydraulic conductivities (K_{sat}) that limit H_2O turnover and O_2 exposure) and a chemical barrier (i.e., residual reductive capacity) to contaminant release. However, many of the previous experiments evaluating the ability of saltstone to chemically reduce and immobilize ^{99}Tc have been conducted using ground saltstone materials as sorbents, a practice that is likely to reduce the moisture level in the material, expose reactive surfaces, enhance exposure to O_2 and alter sorbent properties in an unpredictable manner. Therefore, the objective of the current study was to evaluate contaminant leaching using test methods that accommodate intact saltstone monoliths that better represent the initial physical and chemical state of saltstone within the SDUs.

For the current study, ^{99}Tc-spiked saltstone simulants were produced utilizing formulations defined by Savannah River Remediation LLC (SRR), and subjected to varying curing durations under controlled temperature and humidity conditions chosen to mimic curing conditions within SDU Cell 2B. The grout simulants were compared to actual intact saltstone: cured in place for approximately 20 months and retrieved from SDU Cell 2A. Contaminant mass transfer rates for the saltstone simulants and SDF saltstone samples were assessed using EPA Method 1315, *Mass Transfer Rates of Constituents in Monolithic or Compacted Granular Materials Using a Semi-Dynamic Tank Leaching Procedure*. This method was recently adopted for evaluating contaminant leaching from intact monolithic materials. Contaminant leaching was also evaluated using a novel test method under development at the Savannah River Ecology Laboratory (SREL) known as the Dynamic Leaching Method (DLM). In the DLM testing, a flexible-wall permeameter cell is used to achieve saturated leaching through the intact monolith under an elevated hydraulic gradient in an effort to evaluate the persistence of reductive capacity and subsequent changes in contaminant partitioning occurring within intact saltstone monoliths. Furthermore, changes in the K_{sat} of the test material can also be evaluated over the course of leaching by monitoring changes in flow rate at a fixed hydraulic gradient or changes in pressure at a fixed inlet flow rate. The composition of the chemical leachates from both tests can then be analyzed in an effort to identify potential critical reactions and solid phases controlling contaminant partitioning through geochemical modeling.

For the EPA Method 1315 tests it is important to note that the rate (μg cm^{-2} s^{-1}) of leaching observed for ^{99}Tc, ^{137}Cs and other test constituents decreased over the course of the test, with the cumulative release histories initially conforming to diffusion controlled mechanisms for the purposes of data interpretation and comparison. For the ^{99}Tc-spiked simulants, leaching rates for poorly sorbing contaminants like NO_3^-, as indicated by high effective diffusivities and low leachability indices ($i.e.,\ LI = -\log[D_e]$), were much higher than ^{99}Tc, which was attributed to ^{99}Tc partitioning under reducing conditions. Technetium-99 leaching rates for the spiked saltstone samples also appeared to be

sensitive to curing duration and the reduction capacity of the BFS used in making the grout. Reduction capacity can vary between different BFS sources due to differences in the concentrations of components, in particular sulfur and iron, which are known reductants. Due to supply cessation of a historically utilized BFS, an alternate, or "new", BFS source was sought and approved for use in processing future saltstone batches at SRS. Technetium-99 leaching rates for the intact SDU saltstone samples in the EPA Method 1315 test were extremely similar for the three test samples, but a bit higher than observed for the ^{99}Tc-spiked samples made with the new BFS materials when taking exposed surface area into account. Somewhat surprisingly, the leaching rates for ^{137}Cs from the SDU samples were generally lower than the poorly sorbing contaminant, NO_3^-, with leachability index (*LI*) values that were comparable to those observed for ^{99}Tc. There was some variability in ^{137}Cs leaching rates between the three samples, but this variability may reflect differences in total ^{137}Cs present in the three SDU samples. It is important to note that the "diffusional" release of retained contaminants from monolithic materials observed with EPA Method 1315 reflects a combination of both chemical and physical transport processes, such as dissolution and/or desorption in response to changes in pore solution composition combined with diffusional transport over the course of testing.

For DLM testing, the permeameter system was upgraded to accommodate three test samples at the same time by using the laboratory air compressor to provide the driving force for leaching. The three materials tested include a ^{99}Tc-spiked sample described in Seaman (2015) and two actual radioactive saltstone cores extracted from SDU Cell 2A. The three samples have been leached with an artificial groundwater (AGW) surrogate that has either been degassed to remove O_2 or equilibrated with standard atmosphere. Previous DLM tests indicated that Re was a poor surrogate for ^{99}Tc, with DLM leaching rates similar to that of non-reactive grout constituents, consistent with EPA Method 1315 leaching rates for Re observed in previous studies. The K_{sat} values for the three samples vary greatly and make it difficult to control pore water residence times and maintain constant flow rates. However the DLM results suggest that NO_3^- is being leached at a much higher rate than ^{137}Cs and ^{99}Tc, with ^{137}Cs being leached at a higher rate than ^{99}Tc, consistent with the EPA Method 1315 results. Higher initial ^{99}Tc leaching has been observed for the two SDU Cell 2A samples (in comparison to the laboratory-prepared simulant saltstone samples) but the differences in pore water residence times make it difficult to propose a mechanism to readily explain the phenomenon. Therefore, the DLM system is being modified to provide greater mechanical control of flow rates so that factors such as pore water residence times can be manipulated regardless of the K_{sat} to provide greater experimental control.

List of Tables

List of Figures

List of Acronyms and Abbreviations

AGW	Artificial Groundwater
ANS	American Nuclear Society
ANSI	American National Standards Institute, Inc.
APHA	American Public Health Association
ASTM	American Society for Testing and Materials
BFS	Blast Furnace Slag
DIW	Deionized Water
DLM	Dynamic Leaching Method
DO	Dissolved Oxygen
DOE	Department of Energy
LI	Leachability Index
LLNL	Lawrence Livermore National Laboratory
LSC	Liquid Scintillation Counting
OPC	Ordinary Portland Cement
ORP	Oxidation Reduction Potential
PA	Performance Assessment
psi	pounds per square inch
PV	Pore Volume
SDF	Saltstone Disposal Facility
SDU	Saltstone Disposal Unit
SREL	Savannah River Ecology Laboratory
SRR	Savannah River Remediation LLC
SRS	Savannah River Site
TCLP	Toxic Characteristic Leaching Procedure
UHP	Ultra-High Purity
USEPA	United States Environmental Protection Agency
VZP	Vadose Zone Pore-Water Simulant
XRF	X-Ray Fluorescence

1.0 INTRODUCTION

Reactivity and saturated hydraulic conductivity (K_{sat}) are important factors controlling the rate of weathering and stability of cementitious materials used for the long-term disposal of low-level radioactive wastes. At the Savannah River Site (SRS) chemically reducing materials, such as blast furnace slag (BFS), are added to saltstone grout formulations mixed with low-level radioactive saltwaste materials in order to enhance the attenuation of redox sensitive contaminants, e.g., technetium-99 (^{99}Tc). The persistence of chemically reducing conditions within the grout is an important factor driving long-term risk potential in the Performance Assessment (PA) for the Saltstone Disposal Facility (SDF). The residual reductive capacity of saltstone materials is a function of the grout formulation (i.e., the type and amount of reductive components like BFS), curing conditions, and the degree to which subsequent exposure to dissolved O_2 (DO) is restricted, which is dependent on the material's K_{sat}.

Several studies have demonstrated both the difficulty in reducing pertechnetate (TcO_4^-; i.e., Tc(VII)), the oxidized form of Tc, and the rapid oxidation of reduced Tc (i.e., Tc(IV)) when exposed to even moderate levels of O_2 (Cantrell and Williams, 2013; Kaplan et al., 2011; Kaplan et al., 2008; Almond et al., 2012; Lukens et al., 2005; Ochs et al., 2016). To illustrate the general complexity of the saltstone system, several important redox potentials are provided in Table 1. By convention, standard redox potential reactions are written as reduction reactions. The more positive a given redox potential, the more likely it will be reduced, i.e., proceed to the right. In aqueous systems O_2 and H_2 constrain the limits in terms of achievable levels of oxidation and reduction, respectively. Cements made from BFS are generally considered to be resistant to chemical degradation because of their low permeability (Kurdowski, 2014), a factor that can limit O_2 exposure and inhibit oxidation. Simply based on the redox potentials, it is evident the Re(VII) is more difficult to reduce than Tc(VII), and Tc(VII) is more difficult to reduce than Cr(VI). Dissolved sulfides are generally thought to control the redox environment of pore water in slag rich cements (Atkins and Glasser, 1992; Ochs et al., 2016).

Table 1. Standard redox potential for several important reactions at 25 °C and 1 atm (Stumm and Morgan, 1995).

Reaction	$E°, Volt$
1. $ReO_{4(aq)}^- + 4H^+ + 3e^- \leftrightarrow ReO_{2(s)} + 2H_2O_{(l)}$	-0.55
2. $TcO_{4(aq)}^- + 4H^+ + 3e^- \leftrightarrow TcO_{2(s)} + 2H_2O_{(l)}$	-0.361
3. $Fe^{2+} + 2e^- \leftrightarrow Fe_{(S)}$	-0.44
4. $CrO_4^{2-} + 4H_2O + 3e^- \leftrightarrow Cr(OH)_3 + 5OH^-$	-0.13
5. $2H^+ + 2e^- \leftrightarrow H_2$	0.00
6. $Fe^{3+} + e^- \leftrightarrow Fe^{2+}$	+0.77
7. $Fe(OH)_3 + 3H^+ + e^- \leftrightarrow Fe^{2+} + 3H_2O$	+0.98
8. $O_{2(g)} + 4H^+ + 4e^- \leftrightarrow 2H_2O$	+1.23

Many of the previous experiments evaluating the ability of saltstone to reduce and immobilize Tc have been conducted using ground saltstone materials as sorbents, a practice that is likely to expose new surfaces to oxidation and alter sorbent properties in an unpredictable manner. In addition, controlled H_2 atmospheres have been used as a means of restricting O_2 exposure for studies evaluating contaminant partitioning despite the fact H_2 may serve as a general chemical reductant and may alter the redox speciation of the target contaminants (i.e., Tc, Cr, Pu, etc.) and other important chemical elements (i.e., Fe, Mn, etc.) in the presence and even absence of the test sorbent, i.e., soil, saltstone, etc.

To address such issues, the United States Environmental Protection Agency (USEPA; EPA for short) Method 1315, *Mass Transfer Rates of Constituents in Monolithic or Compacted Granular Materials Using a Semi-Dynamic Tank Leaching Procedure* (USEPA 2013), was developed for evaluating the leaching potential of contaminants found in cementitious materials (Garrabrants et al., 2014; Kosson et al., 2014; Serne et al., 2015). EPA Method 1315 is similar to American National Standards Institute, Inc./American Nuclear Society Method 16.1 (ANSI/ANS16.1), *Measurement of the Leachability of Solidified Low-Level Radioactive Wastes by a Short-Term Test Procedure* (ANSI/ANS, 2003), with the leaching intervals modified to accommodate a more complex interpretation of contaminant release mechanisms. However, both methods are seen as vast improvements over previous tests using size-reduced materials that focus on equilibrium partitioning rather than the rate of contaminant release under physically realistic conditions. The leaching potential of contaminants from solid waste, including "size-reduced" cementitious materials, has previously been evaluated using the batch extraction method defined in EPA Method 1311, *Toxicity Characteristic Leaching Procedure* (TCLP) (USEPA, 1992). The TCLP method was designed to represent the leaching conditions present in a municipal waste landfill scenario. However, contaminant mass transport in monolithic materials is controlled by diffusion through the tortuous pore network combined with the aqueous phase partitioning reactions at the solid/solution interface (i.e., adsorption/desorption, precipitation/dissolution, complexation reactions, etc.).

As noted above, the physical structure of the saltstone material combined with maintaining a high degree of saturation serves as a barrier against exposure to O_2. Grinding saltstone for sorption/desorption tests, and even removal from high humidity environments, may facilitate contaminant oxidation and the consumption of saltstone's inherent reductive capacity. The objective of the current study was to evaluate the leaching behavior of ^{99}Tc and other contaminants from spiked saltstone simulant monoliths in comparison with actual intact saltstone samples collected from Saltstone Disposal Unit (SDU) Cell 2A.

2.0 MATERIALS AND METHODS

2.1 ^{99}Tc Spiked Saltstone Formulation

Two batches of ^{99}Tc-spiked saltstone were produced utilizing Savannah River Remediation LLC (SRR)-prescribed grout formulations, one using Holcim BFS (Holcim US, Inc. Birmingham, AL

35221) and the second using the BFS from the new supplier, Lehigh Cement (Cape Canaveral, FL 32920), a subsidiary of Heidelberg Cement Group. Both batches of saltstone were created using a saltwaste simulant recipe specified by SRR (Table 2) and then subjected to a temperature/humidity curing profile that mimicked the environmental conditions in SDU Cell 2B (Figure 1). The relative concentrations of ^{99}Tc in the saltwaste simulants ($\approx 2 \times 10^4$ pCi mL^{-1}) were consistent with the average concentrations of ^{99}Tc in the Tank 50 feed waste at the SDF (Bannochie, 2012, 2014). The dry feed materials consisted of (1) Class F fly ash (The SEFA Group, Inc. Lexington, SC 29073), (2) Grade 100/120 blast furnace slag (either Holcim or Lehigh), and (3) Type II Portland cement (Holcim US, Inc. Birmingham, AL 35221). The dry feed material ratio was 45% fly ash, 45% BFS and 10% Portland cement

All of the chemicals in Table 2, except for the NaOH solution, were combined with ≈ 0.5 L of deionized water (DIW) in multiple 1-L volumetric polycarbonate flasks depending on the total mass of saltstone being created. The NaOH was then added as a 50% solution. The contaminant spike solution was added to the saltwaste flasks just before making up the solution to its final volume. Spike concentrations are consistent with the average levels of ^{99}Tc found in Tank 50 saltwaste (Bannochie, 2012, 2014). The following day, the required masses of the three powdered grout materials were weighed in three separate containers. The three dry powdered materials were then mixed together in a single bucket. After thorough homogenization of the combined dry powders, the saltwaste simulant solution was slowly added to the dry materials while mixing at 250 rpm for 20 minutes.

The saltwaste solution was added at a water to dry materials ratio of 0.6. After mixing, the ^{99}Tc spiked slurries were poured into several 2” ID x 4” L plastic concrete molds and sealed with plastic lids for curing (Test Mark Industries, Inc.). The plastic concrete molds were then placed in a humidity-controlled curing oven (Model 6105, Caron Products & Services, Inc.) and heated according to the curing profile from SDU Cell 2B (Figure 1).

Table 2. Composition of saltwaste simulant.

Material	Molarity (moles/L)	Mass for 1L (g/L)
Sodium Hydroxide, 50 wt% NaOH	1.594	127.52
Sodium Nitrate, $NaNO_3$	3.159	268.52
Sodium Nitrite, $NaNO_2$	0.368	25.39
Sodium Carbonate, Na_2CO_3	0.176	18.66
Sodium Sulfate, Na_2SO_4	0.059	8.38
Aluminum Nitrate, $Al(NO_3)_3.9H_2O$	0.054	20.25
Sodium Phosphate, $Na_3PO_4.12H_2O$	0.012	4.56

Figure 1. Curing profile for SDU Cell 2B (10.5 ft height).

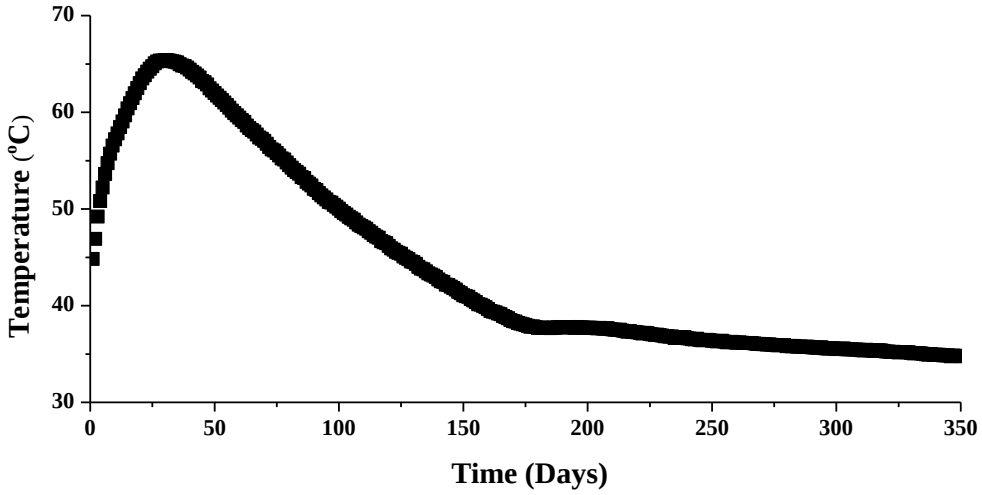

The reductive capacity of the BFS materials used to produce the ^{99}Tc-spiked simulants was determined using the Angus and Glasser (1985) method as modified by Roberts and Kaplan (2009). Approximately 0.5 gm of BFS was weighed into a series of Erlenmeyer flasks and then extracted for four hours using 25 mL of 0.0608 M Ce(IV) in 10% sulfuric acid. The solutions were then titrated with 0.050 M $(NH_4)_2Fe(SO_4)\cdot 6H_2O$ until the redox equivalence point was determined using an oxidation-reduction potential (ORP) electrode. This method proved more accurate than the conventional redox indicator solution, ferroin indicator solution. The titration was calibrated using aliquots of the

unreacted Ce(IV) solution. The reducing equivalents per mass of solid sample (μeq gm^{-1}) was determined from the difference between the total oxidizing equivalents in the Ce(IV) solution and the number of reducing equivalents needed to neutralize the Ce(IV) solution after it reacted with a given BFS sample, divided by the mass of the BFS sample. The reductive capacity and primary constituent concentrations of the two BFS materials is provided in Table 3. The differences on reductive capacity observed between the Holcim and Lehigh BFS materials correspond to the higher Fe and sulfur (S) contents of the Lehigh BFS, elements responsible for providing most of the reductive capacity in such materials.

Table 3. Properties of BFS materials used in making ^{99}Tc-spiked saltstone simulants.

SAMPLE	Reductive Capacity*	Fe**	S	Mn	Ca	Al	Si
	μeq gm^{-1}	mg/kg	mg/kg	mg/kg	mg/kg	mg/kg	mg/kg
Holcim BFS (FY15)	713	1,685	13,934	2,537	234,566	18,324	153,312
Lehigh BFS (Batch 1)	1600	3,504	23,620	1,044	285,232	39,933	126,267
*Angus and Glasser Method (1985)							
**Composition determined by XRF Analysis							

2.2 SDU Cell 2A Core Extraction

Samples of field-emplaced saltstone from the SDF were collected in April-May 2015 to support ongoing SDF PA activities. As summarized in Simner (2016), a set of emplaced saltstone core samples were collected from SDU Cell 2A (SDU-2A) approximately 20 months after the materials had been poured. The core samples were collected using a wet core drilling method. The goal of the sampling effort was to collect saltstone materials that retained the chemical and physical properties of emplaced saltstone for comparison with laboratory-prepared samples that are often used as surrogates for predicting saltstone behavior. The retrieved samples were immediately placed in an inert N_2 environment to prevent oxidation prior to testing. Three of the SDU core samples were included in the current study for comparison, designated SDU-A, SDU-B and SDU-C which corresponds to original sample designations of SDU2A-0931-C-1-U-2, SDU2A-0931-C-1-U-5, and SDU2A-0931-C-2-U-2, respectively. A more thorough description and inventory of the samples from SDU-2A can be found in SRNL-L3100-2015-00108 (SRNL, 2015).

2.3 Contaminant Mass Transfer: EPA Method 1315: Mass Transfer Rates for Monolithic Samples (USEPA, 2013)

EPA Method 1315, a semi-dynamic tank leaching procedure, was used to evaluate contaminant leaching from ^{99}Tc-spiked and SDU-2A saltstone monoliths. EPA Method 1315 is similar to ANSI/ANS16.1 (2003) with modified leaching intervals that potentially allow for a more complex interpretation of processes controlling contaminant release over the course of testing. As discussed previously, EPA Method 1315 and ANSI/ANS16.1 are believed to be more relevant than batch

extraction methods for testing monolithic materials as both procedures more-realistically mimic the physical nature of the intact cementitious material. In the current application of EPA Method 1315, most of the saltstone sample cores (both ^{99}Tc-spiked samples and the three SDU samples) were tested according to the three-dimensional geometry for estimating contaminant release under diffusion controlled release conditions. After curing intervals of three and six months, ^{99}Tc-spiked saltstone monoliths were removed from the curing oven and sectioned for testing. The samples were chosen to exceed the minimum dimensions recommended by the method, i.e., ≥ 5 cm (≈ 2 inches) diameter and length. For EPA Method 1315, the spiked monoliths were sectioned approximately 7.6 cm (≈ 3 inches) above the base and removed from the curing mold immediately before the start of the leaching test. The SDU samples were also sectioned to be of similar size to the ^{99}Tc-spiked samples and provide subsections of a given SDU sample for additional testing, e.g., Dynamic Leaching Method (DLM) testing, chemical analysis, etc. A single ^{99}Tc-spiked sample made using the Lehigh BFS materials was sectioned and tested in the one-dimensional configuration for comparison to current and previous data sets. The relevant properties of the saltstone materials used for EPA Method 1315 testing are provided in Table 4.

Table 4. Physical and chemical properties of ^{99}Tc-spiked saltstone simulants and three saltstone samples from SDU Cell 2A that were tested using EPA Method 1315.

Sample	Curing Duration	BFS Materials	Mass (gm)	1315 Exposed Surface Area (cm^2)	^{99}Tc** ($pCi\ gm^{-1}$)	^{137}Cs*** ($pCi\ gm^{-1}$)
FY16 Data ^{99}Tc Spiked Saltstone						
Tc2	3 Months	Lehigh	267	164	6.7E+03	NA
Tc6	6 Months	Lehigh	261	156	6.7E+03	NA
Tc4 (1D)	6 Months	Lehigh	175	20	6.7E+03	NA
Tc9	3 Months	Holcim	288	168	6.7E+03	NA
SDU Cell 2A Samples						
SDU-A	≈20 Months#	Holcim	272	168	6.4E+03	7.9E+05
SDU-B	≈20 Months#	Holcim	272	168	6.4E+03	4.8E+05
SDU-C	≈20 Months#	Holcim	360	208	6.4E+03	4.9E+05
*Average of test replicates performed under three different atmospheres						
**Based on spike levels for laboratory samples and Tank 50 composition (Bannochie, 2014) for SDU samples						
***Cs-137 levels based on analysis of sectioned SDU samples						
#approximately 20 months curing in SDU Cell 2A plus additional curing after sample collection before testing began						
Sample SDU-A = SDU2A-0931-C-1-U-2						
Sample SDU-B = SDU2A-0931-C-1-U-5						
Sample SDU-C = SDU2A-0931-C-2-U-2						

The terminology adopted by Serne et al. (2015) will be used to refer to the EPA Method 1315 leaching tests, with leachant referring to the starting solution used to interact with the saltstone, and leachate to refer to the resulting solution after contact with saltstone. An artificial groundwater (AGW; see Table 5) surrogate based on routine sampling of non-impacted water table wells on the SRS was used as the leachant (Strom and Kaback, 1992). The mass transfer tests were conducted at room temperature (i.e., 22 ± 2 °C) under ambient laboratory atmosphere. Previous studies detailed in Seaman (2015) demonstrated that ^{99}Tc leaching from monolithic saltstone simulants was generally insensitive

to the test atmosphere. The volume of leachant used in each leaching interval conformed to the liquid-to-surface area ratio (L/A) of 9 ± 1 mL cm^{-2} dictated by EPA Method 1315, and the test leachant was replaced with fresh solution according to the schedule provided in Table 6.

Table 5. Composition of the artificial groundwater (AGW) simulant.

Constituent/Parameter	AGW[a]
pH	5.0
	(mg L^{-1})
Na	1.39
K	0.21
Ca	1.00
Mg	0.66
Cl	5.51
SO_4	0.73

[a]Artificial Groundwater: non-impacted groundwater derived from natural infiltration (Strom and Kaback, 1992)

Table 6. Schedule for fresh leachant renewals for EPA Method 1315.

Interval Label	Interval Duration (h)	Interval Duration (d)	Cumulative Leaching Time (d)
T01	2.0 ± 0.25		0.08
T02	23.0 ± 0.5		1
T03	23.0 ± 0.5		2
T04		5.0 ± 0.1	7
T05		7.0 ± 0.1	14
T06		14.0 ± 0.1	28
T07		14.0 ± 0.1	42
T08		7.0 ± 0.1	49
T09		14.0 ± 0.1	63

The choice of an appropriate leachant solution can have a significant impact of test results. In similar studies Serne et al. (2015) found that contaminant leaching in the presence of a vadose zone pore-water simulant (VZP) derived for Hanford was lower when compared to DIW, which they attributed to precipitates they observed forming at the Cast Stone surface. The precipitate was later identified predominantly as aragonite (a polymorph of calcium carbonate), with some brucite ($Mg(OH)_2$), and possibly calcite ($CaCO_3$) that hindered contaminant diffusion. No such precipitate was observed using an SRS groundwater surrogate in the current study (i.e., AGW), which has a much lower overall ionic strength as well as lower Ca and Mg levels than the Hanford VZP.

Technetium-99 (^{99}Tc) present in EPA leachates was analyzed by liquid scintillation counting (LSC) according to American Society of Testing and Materials (ASTM) D7283-13, *Standard Test Method for Alpha and Beta Activity in Water by Liquid Scintillation*, using a Beckman/Coulter LS6500

(ASTM, 2013). Cesium-137 present in the EPA Method 1315 test leachates from the SDU-2A samples was determined by gamma spectrometry. Nitrate leaching for the SDU and ^{99}Tc-spiked grout samples was monitored using a chromotropic acid test method, American Public Health Association (*APHA) Method-4500-Nitrogen, Standard Methods for the Examination of Water and Wastewater* (APHA, 1997). Analysis of iodine-129 (^{129}I) released from the SDU samples is currently pending.

Leachate Data Analysis

The effective diffusivity, D_e (cm/s^2), for ^{99}Tc, ^{137}Cs and NO_3^- was calculated using the simplified approach outlined in ANSI/ANS-16.1 (ANSI/ANS, 2003):

$$D_e = \pi \left[\frac{a_n / A_0}{\Delta t_n} \right] \left[\frac{V}{S} \right]^2 T \quad [1]$$

where a_n is the quantity of contaminant released during interval n, A_0 is the total quantity of contaminant initially present in the sample being tested, Δt_n is the duration of the n^{th} interval, V is the volume of the sample (cm^3), S is the surface area of the sample (cm^2), and T is the generalized mean square root of the leaching time:

$$T = \left[\frac{\sqrt{t_n} + \sqrt{t_{n-1}}}{2} \right]^2 \quad [2]$$

where t_n is the elapsed time at the end of the current sampling interval and t_{n-1} is the elapsed time at the end of the previous sampling interval. The approach outlined above using the incremental fraction of the contaminant leached during each interval provides an estimate of diffusivity for each sampling interval that is independent of the other sampling intervals, and not subject to any bias that may occur during early sampling times when surficial materials may be released. Additionally, a more-specific solution that accounts for the geometry of the specimen is required when more > 20% of the contaminant has leached from the sample (ANSI/ANS, 2003). When greater than 20% of the initial contaminant inventory has been leached from the sample, as is often seen for NO_3^-, the release data become non-linear with the square root of time due to depletion, and are not included in estimates of diffusivity.

For comparison, the leachability index (*LI*), a unit-less parameter derived from the effective diffusion coefficient, i.e., D_e (cm^2/s), was calculated using the equation presented in Serne et al. (2015):

$$LI_n = -\log[D_e] \quad [3]$$

where LI_n is the leachability index for sampling interval n. The reported *LI* values in the current study reflect the average for all sampling intervals where less than 20% of the initial inventory has been leached. It is important to note that the "diffusional" release of retained contaminants from cementitious waste reflects a combination of both chemical and physical transport processes, such as

dissolution or desorption in response to changes in pore solution composition combined with diffusional transport. A *LI* value of 6 or greater is generally considered the threshold for a given matrix as adequate for immobilization of radioactive wastes (ANSI/ANS, 2003).

2.4 Dynamic Leaching Method

The DLM is based on ASTM D5084-10 (ASTM, 2010) for determining the K_{sat} of cementitious materials using a flexible-wall permeameter to develop the necessary hydraulic gradient and ensure internal flow. Darcy's Law was used to establish the initial leaching conditions:

$$q = \frac{Q}{A} = \frac{K_{sat}\Delta H}{L} \quad [4]$$

where q is the flux density (i.e., volume flowing through a specific cross-sectional area), Q ($cm^3\ sec^{-1}$) is the discharge volume per unit time (i.e., V/t), A is the cross sectional area (cm^2), K_{sat} ($cm\ sec^{-1}$) is the hydraulic conductivity, ΔH is the hydraulic head difference between the column inlet and outlet (i.e., $\Delta H = H_i - H_o$; cm), and L is the length of the column (cm) (Hillel, 1980).

Given a two-inch diameter saltstone monolith (i.e., cross-sectional area of 20.27 cm^2) with a core length of one inch (2.54 cm), and an assumed K_{sat} of 5 x 10^{-9} cm sec^{-1}, the pressure required to achieve a leaching rate of approximately 5 mL per day (i.e., 5.79 x 10^{-5} $cm^3\ sec^{-1}$) can be calculated as:

$$q = \frac{Q}{A} = \frac{5.79\times10^{-5} cm^3 s^{-1}}{20.27\ cm^2} = 2.86 \times 10^{-6} cm\ s^{-1} = \frac{K_{sat}\Delta H}{L} \quad [5]$$

The equation is then solved for ΔH, the required hydraulic gradient in cm of water.

$$\Delta H = \frac{qL}{K_{sat}} = \frac{2.86\times10^{-6} cm\ s^{-1} L}{K_{sat}} = \frac{2.86\times10^{-6} cm\ s^{-1}\times 2.54\ cm}{5\times10^{-9} cm\ s^{-1}} = 1{,}453 cm \quad [6]$$

The hydraulic gradient is then converted to psi.

$$psi = \frac{1{,}453 cm}{70.38\ cm\ psi^{-1}} = 20.61\ psi \quad [7]$$

Changes in the relative K_{sat} during the course of leaching can be estimated using Darcy's equation based on the set hydrostatic pressure at the column inlet and the observed effluent flow rate. The porosity of the ^{99}Tc-spiked sample was determined by the mass loss of water upon heating samples to 105 °C in a laboratory oven, with the heated sample measured repeatedly until the mass change on consecutive days was < 0.5% (Westik et al., 2013). For the current saltstone materials, the average % moisture content ≈ 58%, consistent with other estimates for similar materials (Westik et al., 2013). This was used as an estimate of sample pore volume (PV) for comparing sample monoliths of differing dimensions.

The confining pressure was set at 20-25 psi and the initial driving pressure was set at 12 psi. After flow began, the driving pressure was adjusted as necessary to provide continuous flow. Samples

for chemical analysis were generally collected on a weekly basis. As described above for EPA Method 1315, ^{99}Tc present in effluents was analyzed by LSC, ^{137}Cs was determined by gamma spectrometry, and NO_3^- was monitored using the chromotropic acid test method.

3.0 RESULTS

3.1 EPA Method 1315

A summary of the data for all leaching tests is provided in Appendix A. Plots of the logarithm of cumulative release rate for ^{137}Cs, ^{99}Tc and NO_3^- as a function of the logarithm of leaching time generally yield negative slopes of 0.5 ± 0.15, indicative of a "diffusion" controlled process (USEPA, 2013). Adherence to the linear release model simplifies comparison of different data sets, without necessarily providing information concerning the chemical mechanisms of constituent immobilization and release. However, when greater than 20% of the initial inventory of a specific contaminant has been leached from the sample, the release data generally no longer conform to the diffusional model, and are not included in estimates of diffusivity or the *LI*.

Cesium-137

The measured concentrations of ^{137}Cs in the leachate from the three SDU samples are presented in Figure 2. Two of the three samples yielded very similar leachate concentrations, samples SDU-B and SDU-C. Sample SDU-A yielded ^{137}Cs leachate levels that were somewhat higher than the other two, but the results are consistent with the initial ^{137}Cs levels present in the three SDU samples, with SDU-A having a greater ^{137}Cs content (7.9×10^5 pCi gm^{-1}) than SDU-B (4.8×10^5 pCi gm^{-1}) and SDU-C (4.9×10^5 pCi gm^{-1}) (See Table 4). The reported ^{137}Cs concentration in Tank 50 at the time these materials were poured, third quarter of 2013, was 1.21×10^6 pCi mL^{-1} (Bannochie, 2014). The concentration in the resulting saltstone can be generally estimated by dividing the tank waste concentration by three, i.e., 1.21×10^6 pCi mL^{-1} yields ≈ 4.03×10^5 pCi gm^{-1}, generally consistent the levels of ^{137}Cs present in samples SDU-B and SDU-C.

The ^{137}Cs effective diffusivity values, D_e, ranged from 1.1×10^{-10} to 4.9×10^{-10} cm^2 sec^{-1} with *LI* values of 9.4, 9.9, and 9.3 for SDU-A, SDU-B, and SDU-C, respectively (see Table 7). The ^{137}Cs D_e and *LI* values for three SDU samples illustrates the importance of knowing the initial concentration of contaminant present in the test material in order to properly analyze the leaching results. The *LI* values observed for ^{137}Cs in the current study are generally higher than those reported previously for ordinary Portland cement (LI ≈ 6 to 8.5) (El-Kamash et al., 2011; Goñi et al., 2006; Sayed and Khattab, 2010). Other materials, such as fly ash, zeolites, and slag, are often added to cement materials to enhance ^{137}Cs retention (El-Kamash et al., 2011; Goñi et al., 2006; Sayed and Khattab, 2010). For instance, *LI* values for ^{137}Cs ranged from 8.1 to 12 for ordinary Portland cement blended with various ratios of sand materials. The higher *LI* values observed with the addition of sand results from a reduction in porosity when compared to ordinary Portland cement (OPC) (Sayed and Khattab, 2010).

Cesium generally forms simple aqueous ions and interacts with mineral surfaces through electrostatic ion exchange, with sorption controlled by the presence of similar competing ions, Na, K,

Ca. Additional Si tends to increase the number of cation exchange sites that develop with cement hydration (Ochs et al., 2016).

Figure 2. Leaching results for ^{137}Cs from EPA Method 1315 for three SDU Cell 2A monoliths: (A) leachate concentration, (B) cumulative ^{137}Cs leaching as a function of exposed surface area.

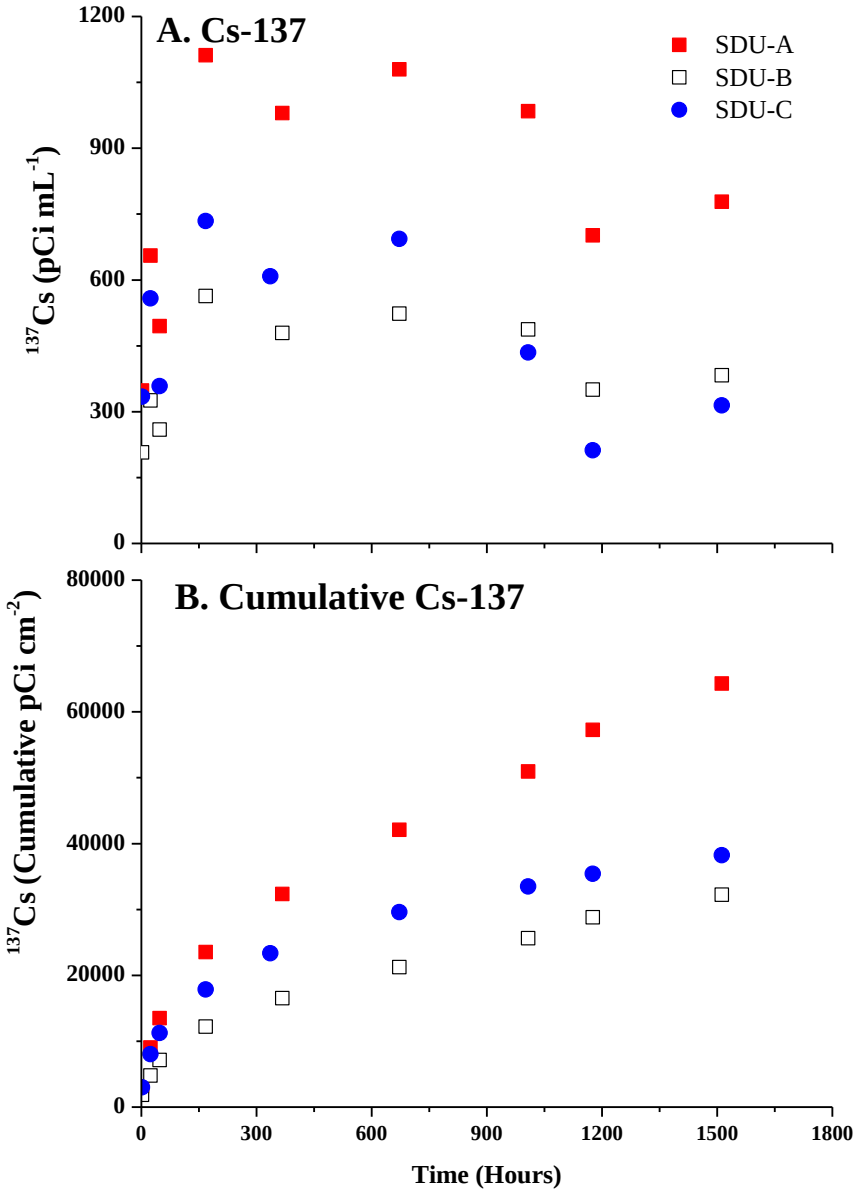

Technetium-99

The EPA Method 1315 ^{99}Tc leaching data for the SDU and ^{99}Tc-spiked samples is presented in Figure 3. The relative ^{99}Tc leaching profiles for the three SDU samples are quite similar (Figure 3A), with much less variability than observed for ^{137}Cs, yielding almost identical cumulative ^{99}Tc leaching profiles (Figure 3C). In contrast the ^{99}Tc leaching date for ^{99}Tc-spiked samples made from the two different BFS source materials are quite different, with higher leaching rates observed for saltstone made from the older Holcim BFS source. In addition the ^{99}Tc leaching data for the Lehigh BFS indicates that extended curing may further enhance ^{99}Tc immobilization.

The difference in ^{99}Tc leaching behavior for the SDU and spiked samples may reflect the greater chemical reduction capacity of the new Lehigh BFS compared to the Holcim BFS used at the time the SDU saltstone was poured (see Table 3), despite the much longer curing time for the SDU materials. The Lehigh BFS apparently has about twice the reductive capacity as the Holcim BFS, which can be attributed to Lehigh's higher Fe and S contents.

It is important to note that the concentrations of ^{99}Tc observed in the current EPA test leachate (6.8×10^{-10} to 4.3×10^{-9} *M* ^{99}Tc) are much lower than those observed by Cantrell and Williams (2013) and Cantrell et al. (2013) for ground ^{99}Tc-spiked saltstone when leached under O_2 free conditions (1.5×10^{-6} *M* ^{99}Tc), which they attributed to reduced precipitate $TcO_2 \cdot 1.6\ H_2O$ based on thermodynamic solubility calculations for their system. The lower ^{99}Tc levels in the current test may be attributed to the lower pH values of the current system (pH ≈ 10-11) compared to the higher pHs (pH ≈ 13-14) of their system, under which the ^{99}Tc precipitate is more soluble.

One of the current ^{99}Tc-spiked monoliths created using the Lehigh BFS was tested using the one-dimensional EPA Method 1315 configuration for comparison with similar tests reported in Seaman (2015) and Seaman et al. (2014). The ^{99}Tc leaching data for the one-dimensional test configuration is also presented in Figure 4 along with the other simulant materials. When presented in terms of exposed surface area, the results for the one-dimensional and three dimensional tests are quite similar for the samples created using the Lehigh BFS (Figure 4B), with less ^{99}Tc leaching than observed for the Holcim test sample.

Figure 3. EPA Method 1315 leaching results for SDU Cell 2A (A and C) materials and ^{99}Tc-spiked saltstone simulants (B and D): leachate concentration (A and B), cumulative ^{99}Tc leaching as a function of exposed surface area (C and D).

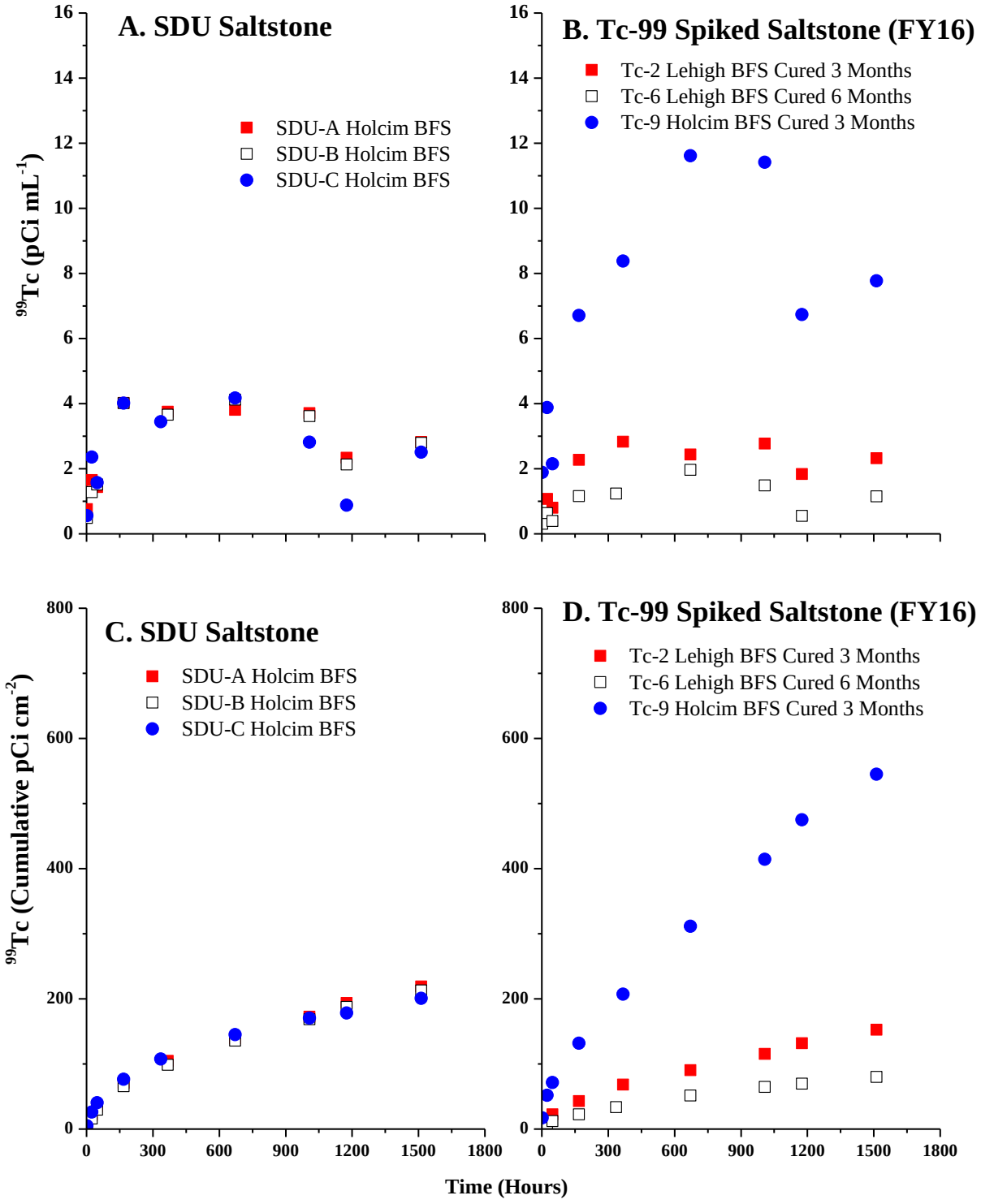

Figure 4. Leaching results for ^{99}Tc-spiked saltstone simulants from EPA Method 1315: (A) leachate concentration, (B) cumulative ^{99}Tc leaching as a function of exposed surface area.

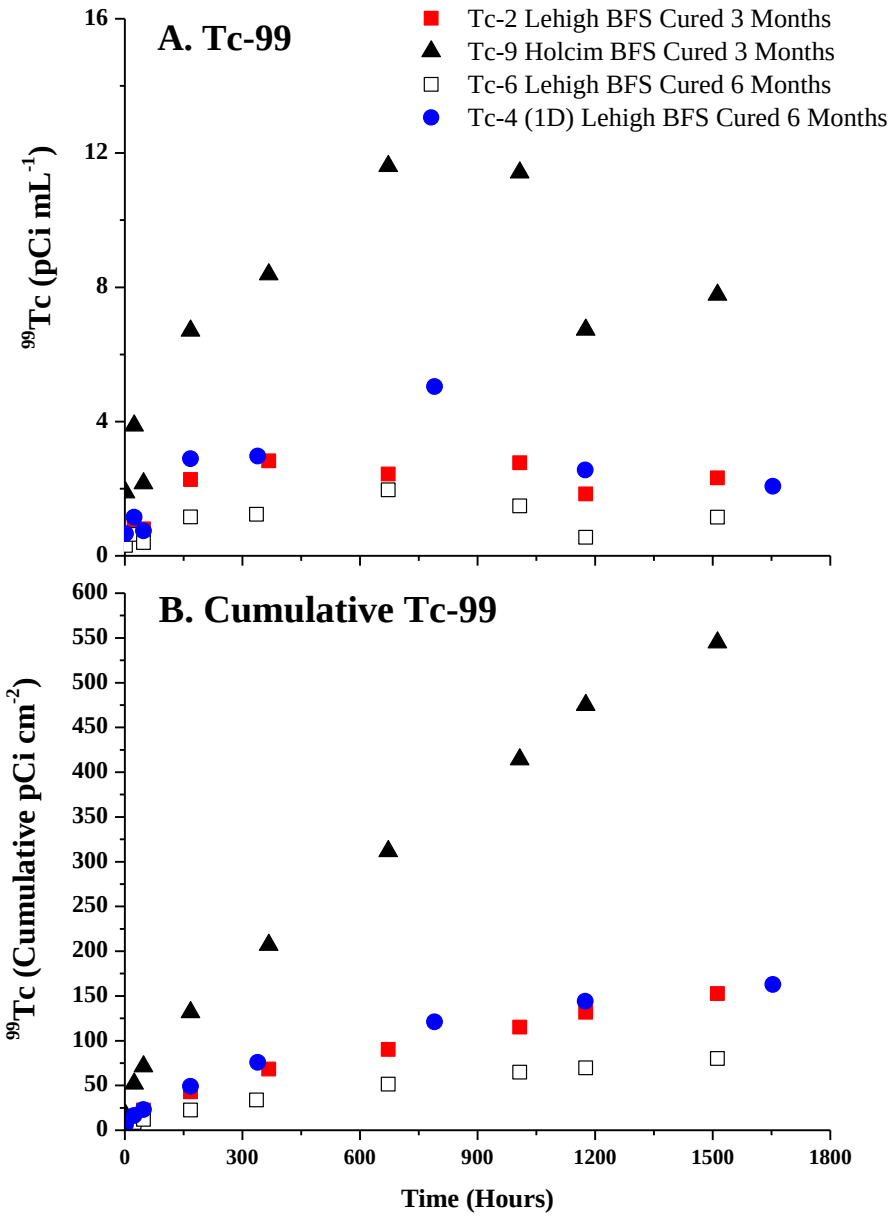

The same EPA Method 1315 one-dimensional data presented in Figures 4 was converted to a molar basis and provided in Figure 5 for direct comparison with one-dimensional ^{99}Tc and Re leaching data from Seaman (2015). Both of the earlier data sets were for saltstone simulants made using the older Holcim BFS. As illustrated in both the leachate (Figure 5A) and the cumulative (Figure 5B) leaching concentrations for ^{99}Tc and Re, the differences in ^{99}Tc leaching behavior for samples generated using the two different BFS materials are far less than the differences observed for the leaching behavior of ^{99}Tc and Re. This indicates that the differences between ^{99}Tc and Re leaching

behavior are indicative of the redox properties of the two elements and not the experimental conditions (i.e., BFS source) of the leaching two tests.

Figure 5. EPA Method 1315 leaching results for Re and ^{99}Tc-spiked saltstone simulants made with two different BFS materials (data presented in terms of µMol concentrations for comparison): (A) leachate concentration, (B) cumulative Re and ^{99}Tc leaching.

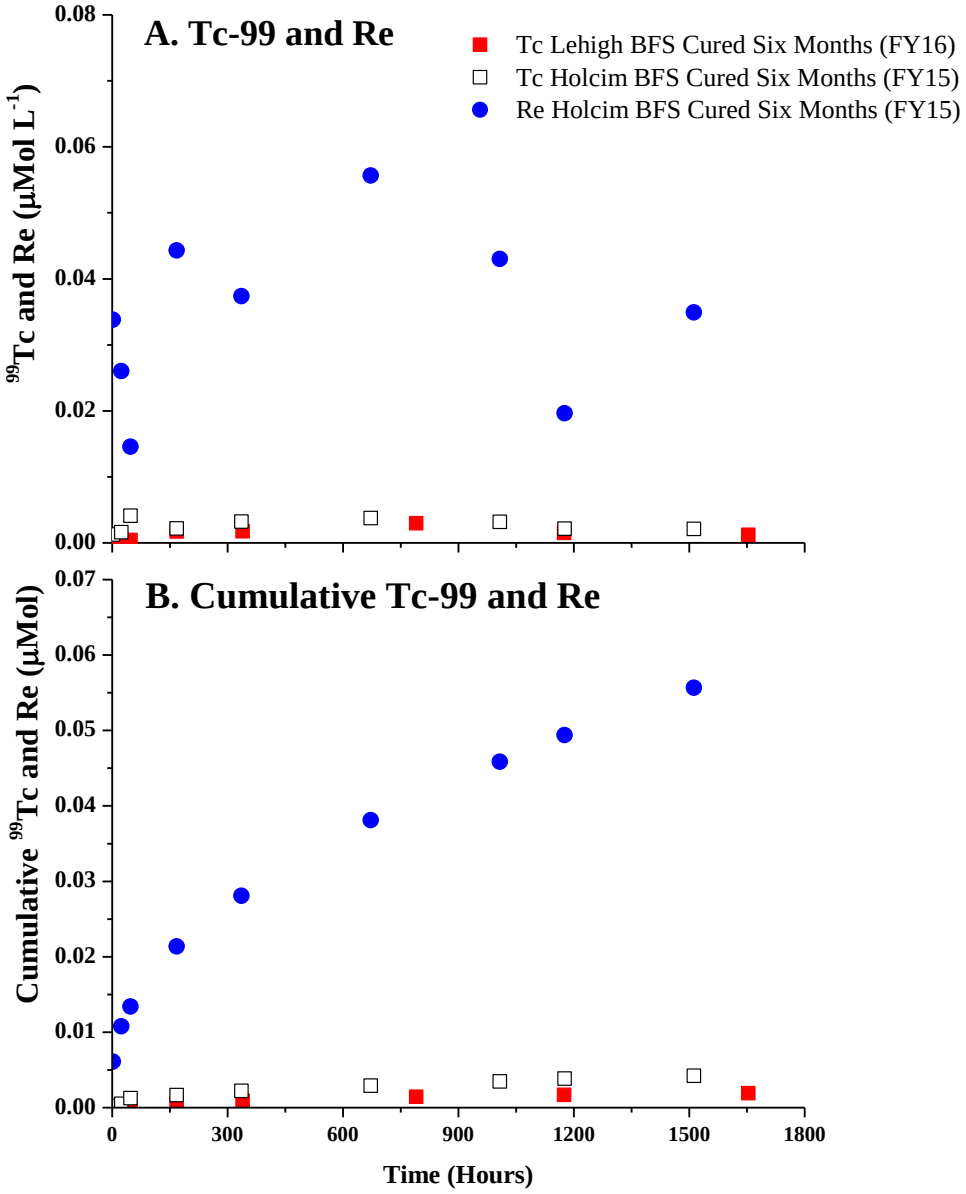

The estimated effective diffusivities (D_e) and LI values for all test constituents present in the SDU and spiked saltstone monoliths are provided in Table 7. Related data from Seaman (2015) and Seaman et al. (2014) are also provided for comparison. As discussed in the earlier reports, the D_e and LI values observed for Re, NO_3^- and stable iodine (^{127}I) are consistent with values observed for "poorly retained constituents" (e.g., Na, NO_3^-, NO_2^-) in laboratory tests of Hanford Cast Stone formulations (Westik et al., 2013; Serne et al., 2015).

As discussed above, the effective diffusivities for ^{137}Cs from the SDU samples ranged from 1.1 x 10^{-10} to 4.9 x 10^{-10} cm^2 s^{-1}, with LI values ranging from 9.3 to 9.9. A LI value of 6 or greater is generally considered the threshold for a given matrix as adequate for immobilization of radioactive wastes (ANSI/ANS, 2003). These LI values are higher than generally observed for ^{137}Cs retention in ordinary Portland cement, but are consistent with values reported for cementitious materials containing BFS and other additives chosen to specifically enhance ^{137}Cs retention (El-Kamash et al., 2011; Goñi et al., 2006; Sayed and Khattab, 2010).

In contrast with the poorly retained constituents (e.g., Re, I, etc.), the effective diffusivities for ^{99}Tc reported by Seaman (2015) ranged from 2.4 x 10^{-10} to 2.8 x 10^{-10} cm^2 s^{-1}, with LIs ranging from 9.7 to 9.9 for ^{99}Tc-spiked saltstone made with Holcim BFS, which is consistent with values observed by Westik et al. (2013) and Serne et al. (2015) for ^{99}Tc in Hanford Cast Stone. In the current study, D_e values for ^{99}Tc-spiked saltstone made with the new BFS materials ranged from 5.7 x 10^{-12} to 3.8 x 10^{-11} cm^2 s^{-1}, with LI values that ranged from 10.4 to 11.3, somewhat better (i.e., slower ^{99}Tc leaching) than reported in Seaman (2015). In part this may reflect the higher reductive capacity of the new BFS material. For the SDU samples made with the Holcim BFS, ^{99}Tc D_e values ranged from 5.2 x 10^{-11} to 6.4 x 10^{-11} cm^2 s^{-1}, with LI values that ranged from 10.2 to 10.3.

Table 7. Summary of effective diffusivities (D_e) and leachability indices (LI) derived from EPA Method 1315.

			^{99}Tc		Re		^{137}Cs		NO_3		^{127}I (stable iodine)	
Sample	Curing Duration	Materials	D_e (cm^2/sec)	LI	D_e (cm^2/sec)	LI	D_e (cm^2/sec)	LI	D_e (cm^2/sec)	LI	D_e (cm^2/sec)	LI
FY15 Data*												
	3 Months	Old BFS (Holcim)	2.4E-10	9.9	3.0E-08	7.6	NA	NA	4.4E-08	7.6	2.9E-08	7.7
	6 Months	Old BFS (Holcim)	2.8E-10	9.7	3.3E-08	7.6	NA	NA	1.6E-08	7.9	3.0E-08	7.7
			^{99}Tc		Re		^{137}Cs		NO_3		^{129}I	
FY16 Data												
Tc2	3 Months	New BFS (Lehigh)	2.6E-11	10.6	NA	NA	NA	NA	4.8E-08	7.5	NA	NA
Tc6	6 Months	New BFS (Lehigh)	5.7E-12	11.3	NA	NA	NA	NA	6.6E-08	7.2	NA	NA
Tc4 (1D)	6 Months	New BFS (Lehigh)	3.8E-11	10.4	NA	NA	NA	NA	2.1E-07	6.7	NA	NA
Tc9	3 Months	Old BFS (Holcim)	3.0E-10	9.6	NA	NA	NA	NA	3.7E-07	6.7	NA	NA
Sample A (SDU A)	20 Months**	Old BFS (Holcim)	6.4E-11	10.2	NA	NA	4.2E-10	9.4	1.3E-08	8.0	Pending	
Sample B (SDU B)	20 Months**	Old BFS (Holcim)	5.8E-11	10.3	NA	NA	1.1E-10	9.9	4.4E-09	8.5	Pending	
Sample C (SDU C)	20 Months**	Old BFS (Holcim)	5.2E-11	10.3	NA	NA	4.9E-10	9.3	5.5E-09	8.5	Pending	

*Reported in Seaman (2015). Reflects the average of three tests (1D configuration) in three different atmospheres

**20 months curing in SDU Cell 2A before sampling

NA Not Applicable

Sample A = SDU2A-0931-C-1-U-2

Sample B = SDU2A-0931-C-1-U-5

Sample C = SDU2A-0931-C-2-U-2

3.3 Dynamic Leaching Method

In earlier studies, Seaman et al. (2014) and Seaman (2015) developed and refined the DLM method to evaluate contaminant partitioning within intact cementitious materials through the use of a flexible-walled permeameter system to achieve steady, saturated leaching through materials with relatively low saturated hydraulic conductivities, i.e., $K_{sat} \leq 1 \times 10^{-9}$ cm sec^{-1}. DLM results clearly demonstrate that Re is a poor analogue for ^{99}Tc, with much greater Re leaching observed from intact samples (Seaman, 2015). In the current study, the DLM system was expanded to accommodate the simultaneous testing of three intact samples. Instead of using a conventional permeameter manifold to control both the confining and leaching pressures, a much simpler expandable test manifold was created with two control valves dedicated to each sample (i.e., a confining and a driving pressure) and a single pressure transducer that can be used to set and monitor each valve, with the required pressures supplied by general compressed laboratory air (Figure 6). A bladder accumulator was added to the system for each test cell to provide a reservoir for the inlet leaching solutions with a flexible membrane that isolates the permeant solution while applying the required driving pressure.

Figure 6. Diagram of the DLM testing apparatus and photograph of laboratory system showing the flex-wall permeameter cell, inlet permeant source within a bladder attenuator, and sample collection outlet.

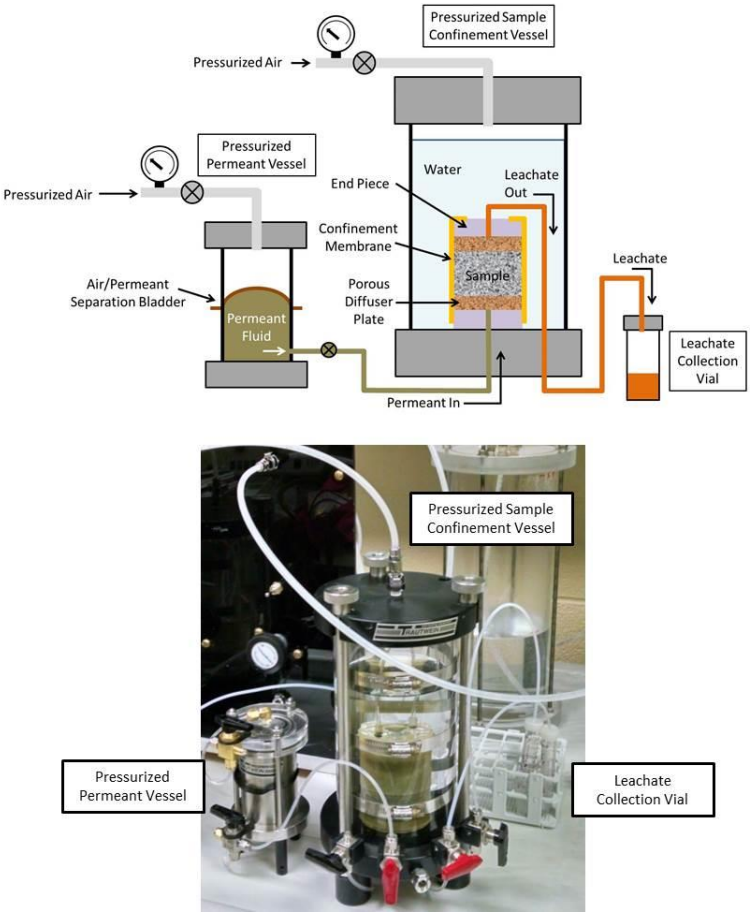

To date, a ^{99}Tc-spiked sample has been continuously leaching with degassed AGW for ≈1 year. In late February 2016, two 5 cm diameter, ≈ 2.5 cm (≈ 1 inch in length) long SDU core sections representing samples SDU-A (SDU2A-0931-C-1-U-2) and SDU-B (SDU2A-0931-C-1-U-5) were added to the test manifold with SDU-A leached with AGW equilibrated with laboratory air and SDU-B leached with degassed AGW. The pore volume for the saltstone monoliths was based on porosity estimates derived from moisture loss at 105 °C for the ^{99}Tc-spiked sample, accounting for ≈ 58% of the monolith volume. While this makes it possible to directly compare data from monolith samples of differing sizes, including the two SDU samples, it is unclear if this measure of porosity is actually indicative of the conductive volume within each of the saltstone samples.

Attempts were made to directly measure the pH, ORP, and DO levels in the DLM effluents after sample collection, factors which control the mobilization of contaminants within saltstone, i.e., ^{137}Cs, ^{129}I, ^{99}Tc, etc. However, it soon became apparent that the three parameters were subject to significant change while the effluent samples were being collected due to the low flow rates. The pH of the samples decreased, likely the result of CO_2 absorption by the alkaline solutions, while the ORP and DO levels increased with storage prior to measurement. In addition, DO electrodes proved unreliable when measuring the highly concentrated, alkaline leachates. To resolve this limitation, the small sample remaining in the effluent tubing was drained into a fresh sample vial and the pH was measured immediately upon collection (Figure 7). Using this method, effluent tubing pH values were typically a full 0.5 to 1.0 unit higher than the pH of the bulk effluent solution in the effluent collection vial. In future DLM tests described below, a flow through system will be used to capture these results before the sample is exposed to the atmosphere.

Figure 7. Effluent pH of DLM samples over the course of leaching. Unreliable pH values are not included.

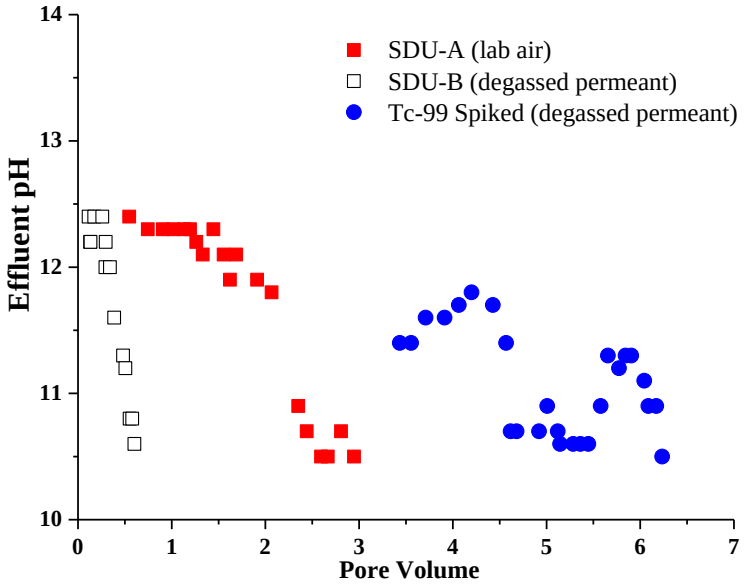

The weathering of cementitious materials depends on their composition, hydration conditions (i.e., curing), and solution chemistries (i.e., composition, DO, CO_2, etc.) to which they are exposed. Figure 8 provides a solubility diagram of important solids thought to control $Tc_{(aq)}$ levels as a function of pH. The four stages of cement degradation, i.e., States I to IV (Ochs et al., 2016), have been superimposed on the Tc solubility diagram. In general, the solubility of chemically reduced Tc phases [i.e., Tc(IV)] decreases as the pH of the cement pore fluid decreases with cement weathering in the absence of Tc oxidation. The initial pH values for SDU-A and SDU-B start at about 12.5 and then decrease steadily over the course of leaching, with the pH decreasing faster for SDU-B. An initial pH of 12.5 is generally consistent with the lower end of the first "stage" (State I) of cement weathering (Figure 8), where alkali metal (Na, K, Cs) leaching occurs. Weathering State I, which usually requires very limited water exchange for conventional cements, is then followed by State II, a period of stable pH (≈ 12.5) where effluent chemistry is generally controlled by the dissolution of Portlandite, $Ca(OH)_2$. For the current samples, the effluent pH values better correspond to State III, where the Ca/Si ratio of the cementitious material decreases with continued leaching (Atkins and Glasser, 1992; Berner, 1992; Ochs et al., 2016). In addition, the decrease in pH observed for the test samples correlates to some degree with an increase in ^{99}Tc leaching (see Figure 11).

Figure 8. Solubility diagram for select Tc phases as a function of pH (25 °C) and a pE (i.e., negative log of electron activity) of 4 with the four weathering stages of cement identified by Berner (1992) and Ochs et al. (2016).

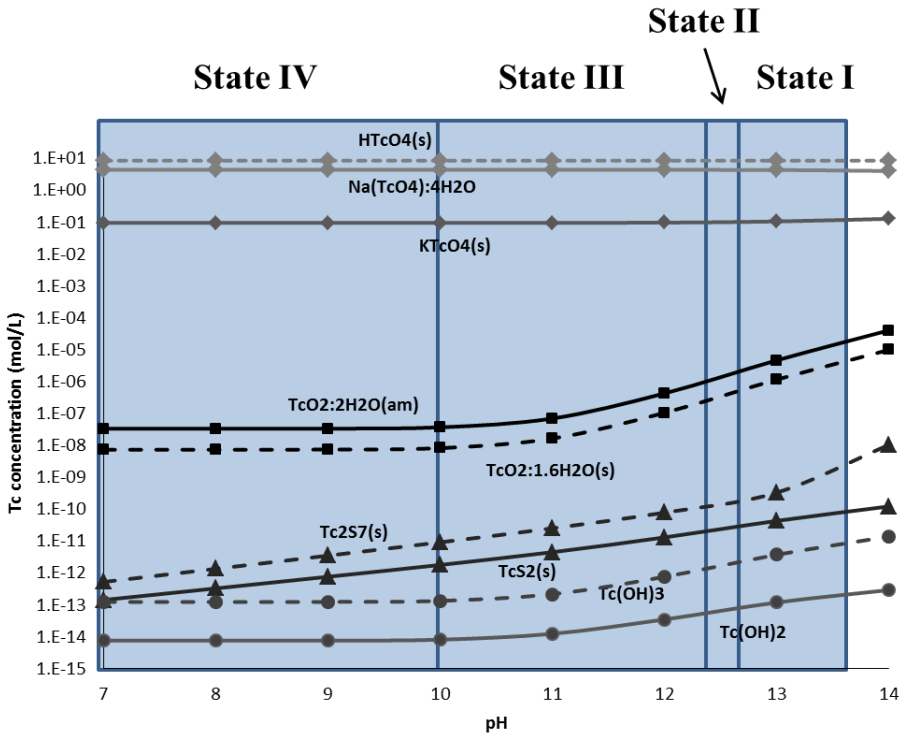

Data generated using PHREEQC-2 and the modified Lawrence Livermore National Laboratory (LLNL) thermodynamic data base (thermo.com.V8.R6.230) prepared by Jim Johnson. The dissolution equation from Cantrell et al. (2013) for TcO_2:1.6H_2O(s) was also included.

The K_{sat} values for the three DLM samples over the course of testing can be seen in Figure 9. After saturation, the initial driving pressure was increased to 12 psi to initiate steady flow. The pressure was then adjusted in increments of 1 psi day^{-1} in an effort to maintain flow at approximately 0.5 to 1 mL per day, while restricting the upper pressure limit to ≈ 25 psi. The K_{sat} for the ^{99}Tc-spiked column has remained fairly stable (≈ 1 x 10^{-9} cm sec^{-1}) over the course of leaching for about 7 pore volumes (assumed to be ≈ 58% of the monolith volume), with only a general decrease in K_{sat} observed over the most recent pore volumes. In contrast, SDU-A displayed a higher initial K_{sat} that decreased over the first two pore volume before stabilizing and even increasing over the last pore volume. And finally the K_{sat} for SDU-B started out at ≈ 1 x 10^{-9} cm sec^{-1} and then decreased to < 1 x 10^{-10} cm sec^{-1}.

Figure 9. Saturated hydraulic conductivity (cm sec^{-1}) of DLM samples over the course of leaching.

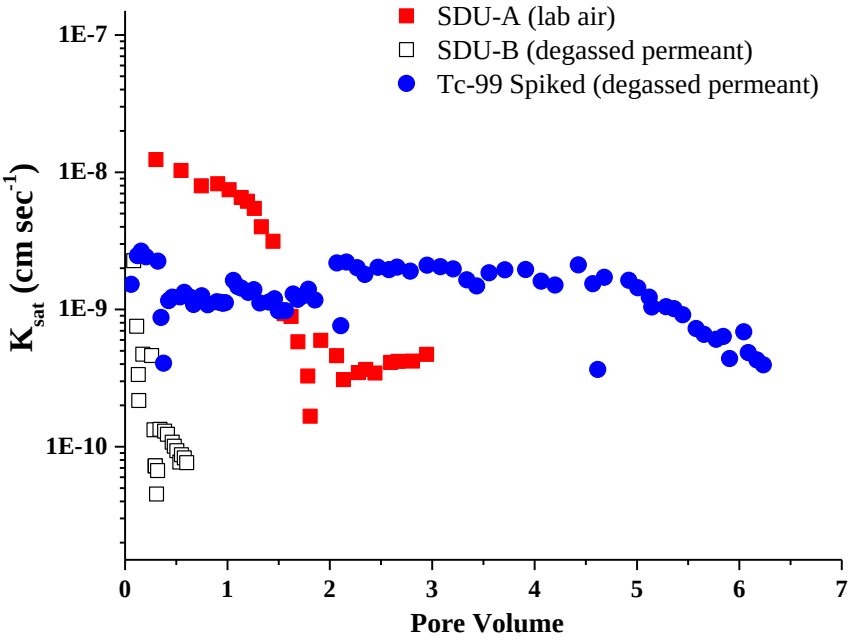

The low K_{sat} values observed for the SDU samples with continued leaching are generally below K_{sat} values (≥ 1 x 10^{-9} cm sec^{-1}) observed for saltstone samples that are tested using standard methods (i.e., ASTM D5084-10) (Seaman et al., 2013; Seaman et al., 2014; Seaman, 2015). While this complicates DLM testing, the lower observed K_{sat} should facilitate maintaining a high degree of saturation and serve as a barrier against exposure to O_2 that can otherwise result in contaminant oxidation and the consumption of saltstone's residual reductive capacity. However, the differences in K_{sat} make it difficult to directly compare data from the three test columns because of their different pore solution residence times, the impact of which will be discussed with respect to contaminant leaching behavior.

The effluent ^{137}Cs levels and cumulative ^{137}Cs extracted over the course of testing for the two SDU samples are provided in Figure 10. Both samples show an initial decrease in ^{137}Cs leaching with a second transient increase ^{137}Cs observed for the SDU-A sample with continued leaching. To date, approximately 8.0 and 3.8 % of the total ^{137}Cs has been leached from SDU-A and SDU-B, respectively. The difference in leaching volume (i.e., < 1 PV for SDU-B compared to 3 PV for SDU-A over the same leaching duration) between the two SDU samples is a reflection in the observed difference in K_{sat}, and the inability to adequately control the driving pressure gradient. The second increase for SDU-A coincides with a precipitous decrease in the K_{sat} of the sample, with ^{137}Cs levels then decreasing as the K_{sat} rebounds. Longer pore water residence times can allow for greater diffusional contaminant exchange from isolated regions of the sample, and greater contaminant release for a kinetically limited sorption reaction (i.e., desorption, dissolution, etc.). Discerning these two possible mechanisms in such complicated physical and chemical systems can be difficult, generally requiring the use of a non-reactive solute tracer.

Figure 10. Cesium-137 leaching from two SDU samples: (A) effluent ^{137}Cs concentration, and (B) cumulative % of ^{137}Cs leached from each column.

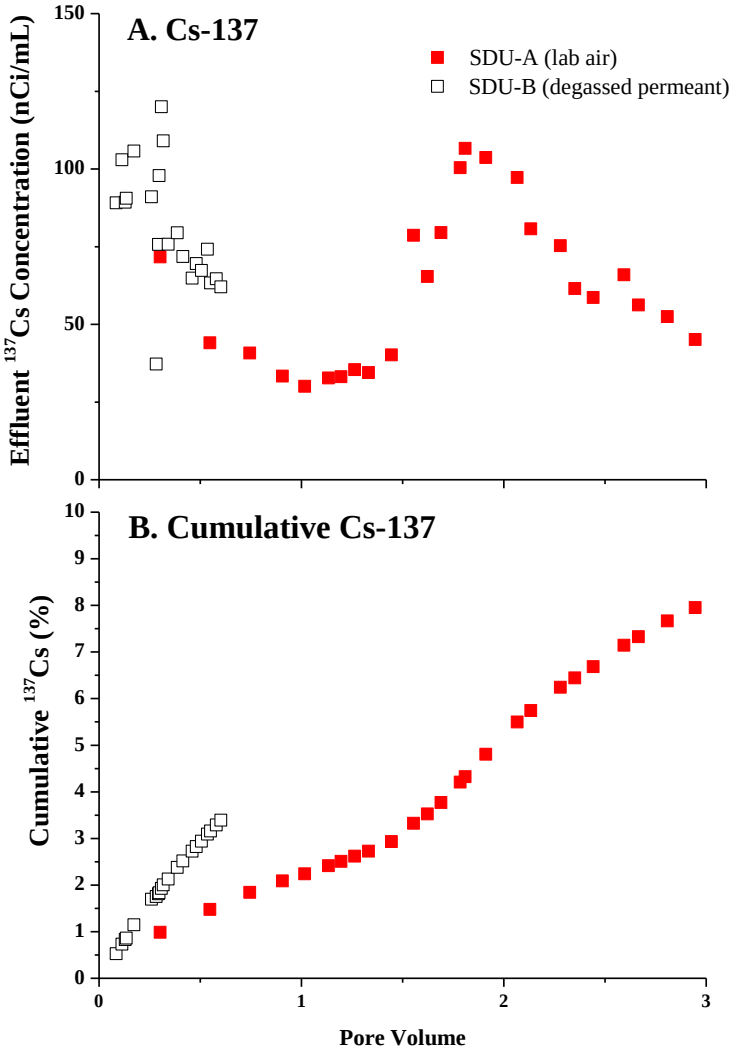

The effluent levels and cumulative ^{99}Tc leached for the two SDU samples and the ^{99}Tc-spiked sample are provided in Figure 11. Technetium-99 leaching from the spiked column was initially quite low and only recently increased dramatically over the last few pore volumes as the K_{sat} gradually decreased. In contrast, the ^{99}Tc leaching rate from sample SDU-A was initially higher than the ^{99}Tc-spiked sample and then decreased over the first two pore volumes. After two pore volumes, however, ^{99}Tc leaching increased at the same time the K_{sat} decreased, somewhat similar to the ^{137}Cs trends observed for SDU-A, but remained high even when K_{sat} rebounded and ^{137}Cs levels decreased. For sample SDU-B, the sample with the lowest K_{sat} (i.e., longest sample residence times), ^{99}Tc leaching has remained high and even increased somewhat over the first pore volume, in contrast to ^{137}Cs behavior for SDU-B. These results suggest that pore water residence time may play some role in ^{99}Tc leaching, but to a lesser degree than observed for ^{137}Cs. Additionally, less cumulative ^{99}Tc has been leached when compared to ^{137}Cs, with 4.9 and 1.9 % of the initial ^{99}Tc has been leached from SDU-A and SDU-B, respectively.

Figure 11. Technetium-99 leaching from the two SDU samples and the ^{99}Tc-spiked saltstone samples: (A) effluent ^{99}Tc concentration, and (B) cumulative % of ^{99}Tc leached from each column.

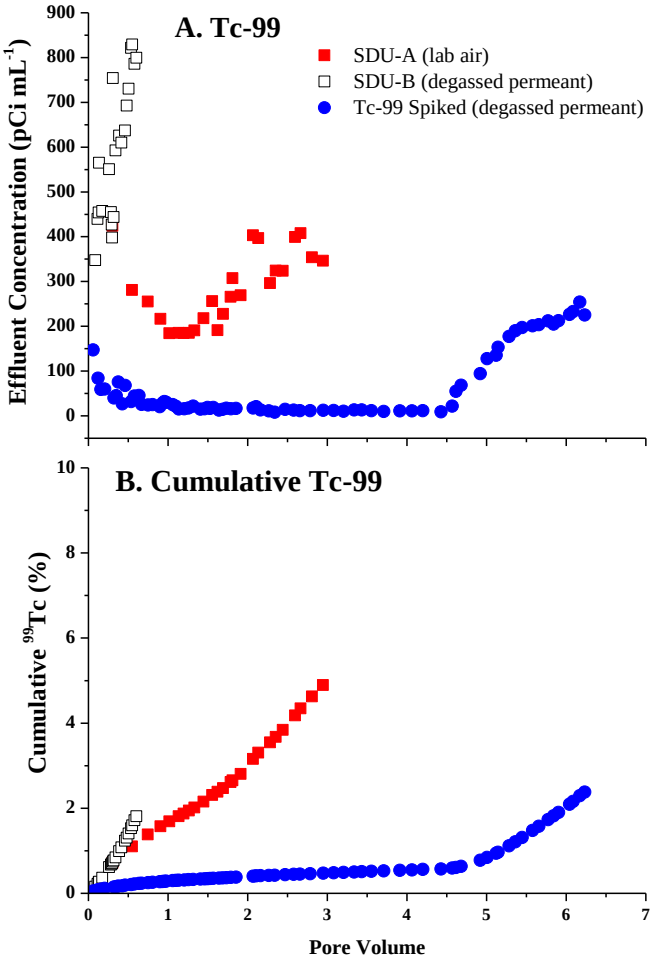

The ^{99}Tc and ^{137}Cs leaching results demonstrate the complex chemical and physical processes controlling contaminant partitioning and immobilization within the saltstone monoliths. Results from SDU-A and the ^{99}Tc-spiked sample (both leached with degassed solutions) suggest that pore water residence times play a large role in controlling contaminant release, either through diffusion of contaminants from non-flowing regions of the sample into the advective stream or a kinetically controlled desorption/dissolution contaminant release mechanism. For the SDU-B sample the ^{99}Tc level has remained high, suggesting that residence time has an impact on ^{99}Tc leaching while the ^{137}Cs levels have fallen, in direct contradiction of a residence time effect.

The cumulative fractions of ^{99}Tc and ^{137}Cs that have been leached from the three samples are provided in Figure 12. As noted above, less of the initial ^{99}Tc when compared to ^{137}Cs has been leached from the two SDU columns, with an even smaller fraction of the total ^{99}Tc (≈ 2%) extracted from the ^{99}Tc-spiked saltstone.

Figure 12. Cumulative % of ^{99}Tc (A) and ^{137}Cs (B) leached from each sample.

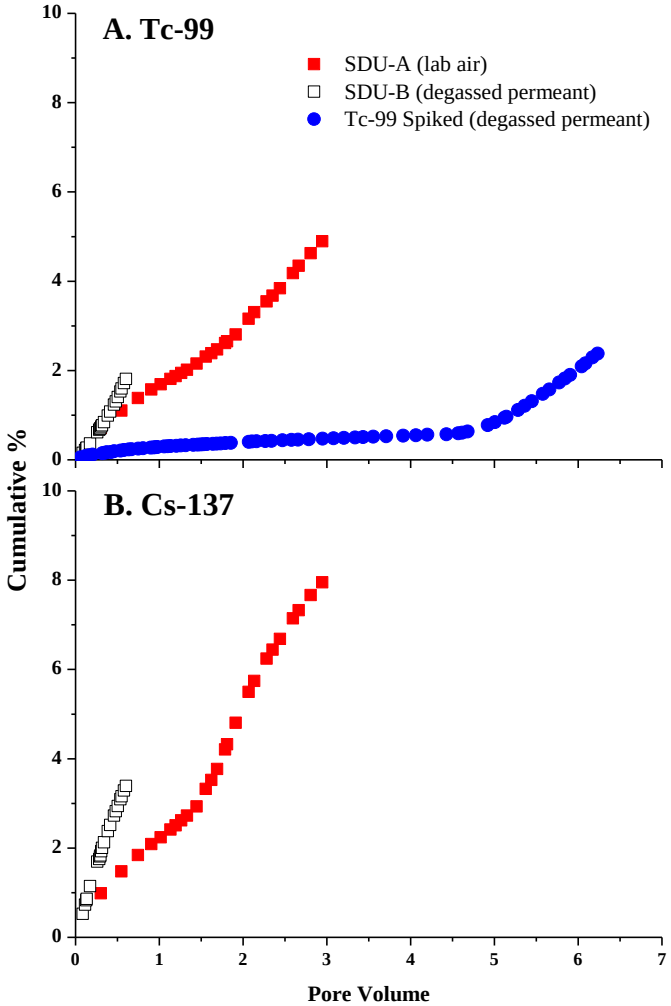

These results for ^{99}Tc and ^{137}Cs are in stark contrast to the leaching pattern observed for NO_3^- (Figure 13), which is generally considered to be poorly retained with cementitious materials. For SDU-

A, the NO_3^- leaching pattern is quite similar to that of ^{137}Cs, despite much higher cumulative levels of NO_3^- leached over the course of the test (Figure 13B). The NO_3^- leaching for SDU-A is also similar to the leaching behavior of ^{99}Tc (at much lower cumulative levels than ^{99}Tc), but the secondary increase is transient for NO_3^- (same as ^{137}Cs), while the ^{99}Tc level has remained elevated. For SDU-B, the NO_3^- leaching pattern is similar to that of ^{137}Cs as well, i.e., generally decreasing since the onset of leaching, while the ^{99}Tc concentration has remained high. For the ^{99}Tc-spiked column, the recent increase in NO_3^- leaching is generally similar that observed for ^{99}Tc.

Figure 13. Nitrate (NO_3^-) leaching from the two SDU samples and the ^{99}Tc-spiked saltstone samples: (A) effluent NO_3^- concentration, and (B) cumulative % of NO_3^- leached from each sample.

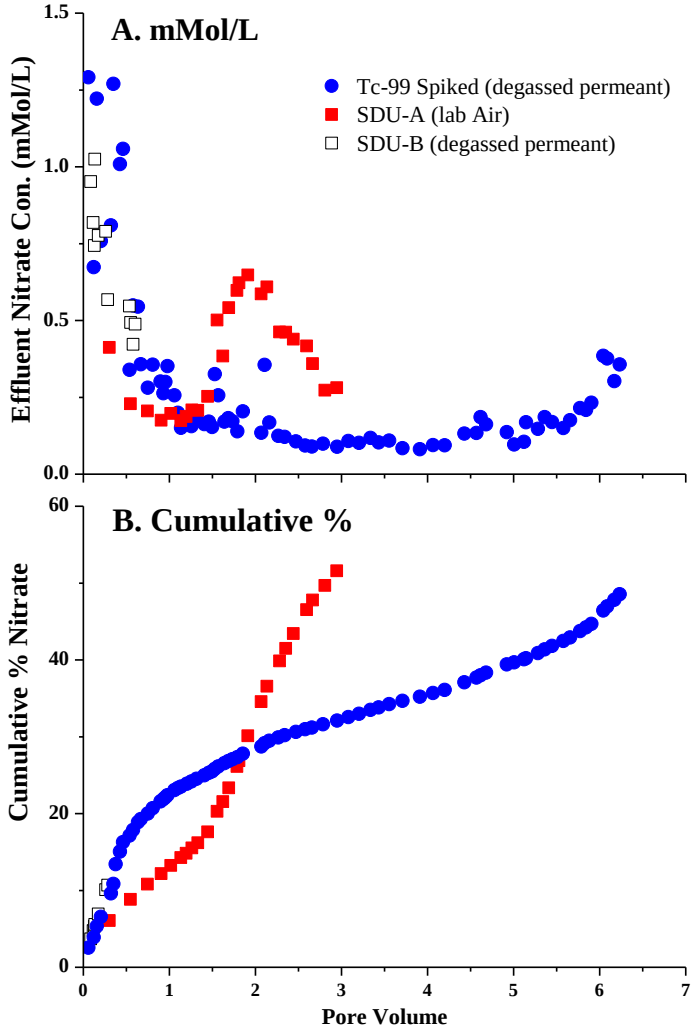

4.0 Discussion

As noted in the introduction, laboratory batch extraction methods for evaluating contaminant release from monolithic materials such as grouts and concrete are somewhat unrealistic because such methods fail to account for the inherent physical structure of the materials, properties that control saturation and exposure to water and oxidizing agents (i.e., O_2) that impact constituent partitioning. Laboratory methods for evaluating the inherent reductive capacity of such materials suffer from similar limitations which also make it difficult to produce consistent results that are relevant to large-scale disposal systems.

EPA Method 1315 results were generally consistent for ^{99}Tc-spiked saltstone simulants and saltstone samples collected from SDU Cell 2A. Differences in leaching rates for SDU and simulant samples generally suggest that the chemical reductive capacity of the BFS and the curing duration are important factors controlling ^{99}Tc immobilization. Furthermore, results for the SDU samples displayed significant ^{137}Cs ($LI \approx 9.3$-9.9) immobilization capacity when compared to the mobile contaminant, NO_3^-, which can be attributed to the greater binding affinity for alkaline earth metals of grout materials made from Portland cement combined with BFS and fly ash.

DLM tests demonstrated the ability to maintain continuous saturated flow through SDU samples as a means of evaluating the reactions occurring within the intact materials. However, flow rates and residence times were quite different for the three test samples and varied to some degree for a given sample, with generally lower K_{sat} values observed for the SDU samples when compared to saltstone simulants. Furthermore, the low flow rates made it difficult to monitor the geochemical properties of the effluents that are critical to evaluating the mechanisms controlling contaminant partitioning (i.e., pH, DO, ORP, etc.), especially for ^{99}Tc because of its tendency to oxidize when exposed to even limited DO levels. Although efforts were made to control the level of DO present in the permeant solutions, it is difficult to draw definitive conclusions regarding the possible impact of DO based on the limited effluent data set.

To address these issues a modified DLM system is under development. Instead of relying on applied pressure gradients that require constant adjustment to achieve steady flow, the modified system uses high-precision mechanical pumps to provide a constant flow rate (i.e., 1-2 mL day^{-1}) while the resulting pressure gradient will be monitored continuously as an indicator of changes in K_{sat}. This will provide better experimental control so that factors such as pore water residence times can be controlled and flow through sensors can be used to monitor effluent chemistry, i.e., pH, DO, ORP. In addition, a much broader range of effluent constituents will be monitored in an effort to identify and monitor solid-phase transitions that control ^{99}Tc solubility and leaching within saltstone.

5.0 References

Almond, P.M., D.I. Kaplan, C.A. Langton, D.B. Stefanko, W.A. Spencer, A. Hatfield, and Y. Arai (2012) Method Evaluation and Field Sample Measurements for the Rate of Movement of the Oxidation Front in Saltstone. SRNL, Aiken, SC 29808.

Angus M.J., Glasser F.P. (1985) The chemical environment in cement matrices. Mat. Res. Soc. Symp. Proc. 50:547-556.

ANSI/ANS (2003) ANSI/ANS-16.1-2003, R2008 (R=Reaffirmed): Measurement of the Leachability of Solidified Low-Level Radioactive Wastes by a Short-Term Test Procedure. American Nuclear Society/ American National Standards Institute, Inc.

APHA (1997) Method-4500-Nitrogen. Standard Methods for the Examination of Water and Wastewater, Washington, DC 20005.

ASTM (2013) ASTM D7283-13 Standard Test Method for Alpha and Beta Activity in Water by Liquid Scintillation, West Conshohocken, PA.

ASTM (2010) ASTM D5084-10: Standard Test Methods for Measurement of Hydraulic Conductivity of Saturated Porous Materials Using a Flexible Wall Permeameter, ASTM International, West Conshohocken, PA 19428-2959.

Atkins, M., and Glasser, F. P. (1992) Application of portland cement-based materials to radioactive waste immobilization. Waste Management 12, 105-131.

Bannochie C.J. (2012) Results of the Third Quarter 2012 Tank 50 WAC Slurry Sample: Chemical and Radionuclide Contaminants, Savannah River National Laboratory, Aiken, SC 29808. SRNL-STI-2013-00651, Rev. 1.

Bannochie, C. J. (2014) Results of the Third Quarter 2013 Tank 50 WAC Slurry Sample: Chemical and Radionuclide Contaminants. Savannah River National Laboratory, Aiken, SC 29808. SRNL-STI-2012-00621.

Berner, U. R. (1992) Evolution of pore water chemistry during degradation of cement in a radioactive waste repository environment. Waste Management 12, 201-219.

Cantrell, K.J. and Williams B.D. (2013) Solubility control of technetium release from Saltstone by $TcO_2 \cdot xH_2O$. J. Nuclear Materials 437:424-431. DOI: http://dx.doi.org/10.1016/j.jnucmat.2013.02.049.

Cantrell K.J., Carroll K.C., Buck E.C., Neiner D., Geiszler K.N. (2013) Single-pass flow-through test elucidation of weathering behavior and evaluation of contaminant release models for Hanford tank residual radioactive waste. Applied Geochemistry 28:119-127.

El-Kamash, A.M., Sami, N.M., and El-Dessouky, M.I. (2011) Leaching Behavior of ^{137}Cs and ^{60}Co Radionuclides from Stabilized Waste Matrices. International Journal of Environmental Engineering Science 2, 199-211.

Garrabrants A.C., Kosson D.S., DeLapp R., van der Sloot H.A. (2014) Effect of coal combustion fly ash use in concrete on the mass transport release of constituents of potential concern. Chemosphere 103:131-139. DOI: http://dx.doi.org/10.1016/j.chemosphere.2013.11.048.

Goñi, S., Guerrero, A., and Lorenzo, M. P. (2006) Efficiency of fly ash belite cement and zeolite matrices for immobilizing cesium *Journal of Hazardous Materials B137 (2006) 1608–1617.*

Hillel, D. (1980) "Fundamentals of soil physics," Academic Press, New York.

Kaplan D.I., Lilley M.S., Almond P.M., Powell B.A. (2011) Long-term Technetium Interactions with Reducing Cementitious Materials, Savannah River National Laboratory, Aiken, SC. SRNL-STI-2010-00668.

Kaplan D.I., Roberts K., Shine G., Grogan K., Fjeld R., Seaman J.C. (2008) Range and distribution of technetium Kd values in the SRS subsurface environment, Savannah River National Laboratory, Aiken, SC. SRNS-STI-2008-00286, Rev. 1.

Kosson D.S., Garrabrants A.C., DeLapp R., van der Sloot H.A. (2014) pH-dependent leaching of constituents of potential concern from concrete materials containing coal combustion fly ash. Chemosphere 103:140-147. DOI: http://dx.doi.org/10.1016/j.chemosphere.2013.11.049.

Kurdowski, W. (2014) "Cement and Concrete Chemistry," Springer.

Lukens W.W., Bucher J.J., Shuh D.K., Edelstein N.M. (2005) Evolution of technetium speciation in reducing grout Environ. Sci. & Technol. 39:8064-8070.

Ochs, M., Mallants, D., and Wang, L. (2016) "Radionuclide and Metal Sorption on Cement and Concrete," Springer, New York.

Roberts, K.A., and D.I. Kaplan (2009) Reduction Capacity of Saltstone and Saltstone Components. Savannah River National Laboratory, Aiken, SC, SRNL-STI-2009-00637.

Sayed, M. S., and Khattab, M. M. (2010) Immobilization of Liquid Radioactive Wastes by Hardened Blended Cement - White Sand Pastes. J. American Science 6, 334-341.

Serne R.J., J.H. Westsik Jr., Williams B.D., Jung H.B., Wang G. (2015) Extended Leach Testing of Simulated LAW Cast Stone Monoliths, Pacific Northwest National Laboratory, PNNL-24297 RPT-SLAW-001 Rev 0, Richland, WA.

Seaman J.C., H.S. Chang, and S Buettner (2014) Chemical and Physical Properties of Saltstone as Impacted by Curing Duration, SREL Doc. R-14-0006, ver. 1.0. Submitted to SRR September 23, 2014.

Seaman, J.C., H.S. Chang, and S.W. Buettner (2013) Comparison of Hydraulic Property Measurement Techniques for Simulated Saltstone. SREL Doc. R-13-0006, ver. 1.0. Submitted to SRR September 4, 2013.

Seaman, J.C. (2015) Chemical and Physical Properties of ^{99}Tc-Spiked Saltstone as Impacted by Curing Duration and Leaching Atmosphere. SREL Doc. R-15-0003, Submitted to SRR October 1, 2015.

Simner, S. P. (2016) Property Data for Core Samples Extracted from SDU Cell 2A. Savannah River Remediation. SRR-CWDA-2016-00051.

SRNL (2015) Appendix 1: Core Section Designation for Chemical and Physical Analysis. SRNL-L3100-2015-00108, Rev. 0.

Strom R.N., Kaback D.S. (1992) SRP Baseline Hydrogeologic Investigation: Aquifer Characterization Groundwater Geochemistry of the Savannah River Site and Vicinity (U), Westinghouse Savannah River Company, Environmental Sciences Section, Aiken, SC. pp. 98.

Stumm W., Morgan J.J. (1995) Aquatic chemistry: An introduction emphasizing chemical equilibria in natural waters. 3rd ed. Wiley-Interscience, New York.

USEPA. (1992) Method 1311: Toxicity Characteristic Leaching Procedure, Test Methods for Evaluating Solid Waste, Physical/Chemical Methods (SW-846), Office of Solid Waste, Washington, DC.

USEPA (2007) Method 6020A, Rev. 1. Inductively coupled plasma-mass spectrometry, Test Methods for Evaluating Solid Waste, Physical/Chemical Methods (SW-846), Office of Solid Waste, Washington, DC.

USEPA (2013) Method 1315, Mass transfer rates of constituents in monolithic or compacted granular materials using a semi-dynamic tank leaching procedure. Test Methods for Evaluating Solid Waste, Physical/Chemical Methods (SW-846), Office of Solid Waste, Washington, DC.

Westsik J.H., Jr, G.F. Piepel, M.J. Lindberg, P.G. Heasler, T.M. Mercier, RL Russell, A. Cozzi, W.E. Daniel Jr, R.E. Eibling, E.K. Hansen, M.M. Reigel, and D.J. Swanberg (2013) Supplemental Immobilization of Hanford Low-Activity Waste: Cast Stone Screening Tests. PNNL-22747, Pacific Northwest National Laboratory, Richland, WA.

Appendix A1: Data Summary for EPA Method 1315
^{99}Tc Spiked Saltstone

Monolith Sample Designation:			Tc2
BFS Source:			Lehigh
Curing Duration:			3 Months
Sample Volume (mL):			1477
Sample No.	Days	pH	^{99}Tc (pCi mL^{-1})
1	0.08	ND	0.62
2	1	11.04	1.07
3	2	10.83	0.80
4	7	11.09	2.27
5	15.3	11.21	2.83
6	28	11.28	2.43
7	42	11.34	2.77
8	49	11.03	1.84
9	63	11.20	2.32

Monolith Sample Designation:			Tc6
BFS Source:			Lehigh
Curing Duration:			6 Months
Sample Volume (mL):			1514
Sample No.	Days	pH	^{99}Tc (pCi mL^{-1})
1	0.08	10.49	0.31
2	1	10.94	0.64
3	2	10.80	0.40
4	7	11.12	1.15
5	14	ND	1.23
6	28	11.24	1.97
7	42	11.24	1.49
8	49	10.96	0.55
9	63	11.03	1.15

Monolith Sample Designation:			Tc4
BFS Source:			Lehigh
Curing Duration:			6 Months
Sample Volume (mL):			180
Sample No.	Days	pH	^{99}Tc (pCi mL^{-1})
1	0.08	10.70	0.66
2	1	11.00	1.15
3	2	10.90	0.75
4	7	10.49	2.89
5	14.1	10.45	2.97
6	32.9	10.60	5.04
7	49.0	10.50	2.55
8	68.9	10.30	2.07
9	ND	ND	ND

Monolith Sample Designation:			Tc9
BFS Source:			Holcim
Curing Duration:			3 Months
Sample Volume (mL):			1477
Sample No.	Days	pH	^{99}Tc (pCi mL^{-1})
1	0.08	ND	1.89
2	1	11.12	3.88
3	2	11.11	2.15
4	7	11.33	6.71
5	15.3	11.51	8.38
6	28	11.64	11.61
7	42	11.72	11.42
8	49	11.53	6.74
9	63	11.47	7.77

ND = Not determined

SDU Cell 2A Saltstone Samples

Monolith Sample Designation:		SDU-A = SDU2A-0931-C-1-U-2		
BFS Source:				Holcim
Curing Duration:				20+ Months
Sample Volume (mL):				1514
Sample No.	Days	pH	^{99}Tc (pCi mL^{-1})	137Cs (pCi mL^{-1})
1	0.08	ND	0.76	348
2	1	11.24	1.65	655
3	2	11.11	1.44	495
4	7	11.37	4.02	1112
5	15.3	11.44	3.75	980
6	28	11.40	3.81	1080
7	42	11.41	3.71	984
8	49	11.10	2.33	701
9	63	11.19	2.82	778
Monolith Sample Designation:		SDU-B = SDU2A-0931-C-1-U-5		
BFS Source:				Holcim
Curing Duration:				20+ Months
Sample Volume (mL):				1514
Sample No.	Days	pH	^{99}Tc (pCi mL^{-1})	137Cs (pCi mL^{-1})
1	0.08	ND	0.48	207
2	1	11.24	1.28	326
3	2	11.10	1.51	259
4	7	11.37	4.02	563
5	15.3	11.45	3.66	479
6	28.0	11.40	4.12	523
7	42.0	11.45	3.62	488
8	49.0	11.10	2.13	350
9	63	11.21	2.80	383
Monolith Sample Designation:		SDU-C = SDU2A-0931-C-2-U-2		
BFS Source:				Holcim
Curing Duration:				20+ Months
Sample Volume (mL):				1872
Sample No.	Days	pH	^{99}Tc (pCi mL^{-1})	137Cs (pCi mL^{-1})
1	0.08	11.13	0.55	334
2	1	11.36	2.36	558
3	2	11.00	1.57	358
4	7	11.46	4.01	734
5	14	ND	3.44	608
6	28	11.42	4.17	693
7	42	11.35	2.82	435
8	49	11.13	0.88	212
9	63	11.10	2.51	314
ND = Not determined				